

## RESEARCH ARTICLE

# Kingfisher feathers – colouration by pigments, spongy nanostructures and thin films

Doekele G. Stavenga\*, Jan Tinbergen, Hein L. Leertouwer and Bodo D. Wilts

Computational Physics, Zernike Institute for Advanced Materials, University of Groningen, NL-9747 AG Groningen, The Netherlands

\*Author for correspondence (D.G.Stavenga@rug.nl)

Accepted 5 September 2011

### SUMMARY

The colours of the common kingfisher, *Alcedo atthis*, reside in the barbs of the three main types of feather: the orange breast feathers, the cyan back feathers and the blue tail feathers. Scanning electron microscopy showed that the orange barbs contain small pigment granules. The cyan and blue barbs contain spongy nanostructures with slightly different dimensions, causing different reflectance spectra. Imaging scatterometry showed that the pigmented barbs create a diffuse orange scattering and the spongy barb structures create iridescence. The extent of the angle-dependent light scattering increases with decreasing wavelength. All barbs have a cortical envelope with a thickness of a few micrometres. The reflectance spectra of the cortex of the barbs show oscillations when measured from small areas, but when measured from larger areas the spectra become wavelength independent. This can be directly understood with thin film modelling, assuming a somewhat variable cortex thickness. The cortex reflectance appears to be small but not negligible with respect to the pigmentary and structural barb reflectance.

Key words: iridescence, scattering, feather barbs, feather cortex, pigment granules.

### INTRODUCTION

The plumage of many birds is highly attractive, especially when the feathers are patterned in strongly contrasting colours. A particularly striking bird is the common kingfisher, *Alcedo atthis* L., which shows a strong contrast between the orange feathers of the breast, the cyan feathers of the back and the blue tail feathers. Here, we investigated the anatomical basis and the optical characteristics of the kingfisher's feathers.

Orange colours are generally caused by pigments that selectively absorb short-wavelength light. When these pigments are embedded in a diffusive medium, only the long-wavelength part of incident broad-band light is reflected and scattered. In contrast, blue or green animal colouration is virtually always due to periodic structures that reflect and scatter incident light of a restricted short-wavelength range (Srinivasarao, 1999; Vukusic and Sambles, 2003; Kinoshita and Yoshioka, 2005; Prum, 2006). Pigmentary and structural colouration are often found simultaneously, not only in birds but also in many other animals, for example butterflies, beetles and lizards (Kinoshita, 2008). Birds possess various pigment classes, for instance carotenoids, pterins, porphyrins, psittacofulvins and melanins (McGraw, 2006; Hill and McGraw, 2006), and various mechanisms of structural colouration, namely thin films, multilayers, photonic crystals, keratin spongy nanostructures and nanofibres (e.g. Durrer, 1977; Shawkey et al., 2003; Shawkey et al., 2006; Yoshioka et al., 2007; Doucet and Meadows, 2009; Prum et al., 2009; Stavenga et al., 2010; D'Alba et al., 2011). The predominant location of colouration is the feathers, often either the barbs or the barbules. The colour of *A. atthis* feathers has been attributed to spectrally selective pigment and to a spongy nanostructure in the barbs (Finger, 1995). Here, we show that the barb cortex, which acts as a thin film of varying thickness, also contributes noticeably to the reflectance spectra.

### MATERIALS AND METHODS

The photograph of *Alcedo atthis* shown in Fig. 1A was taken by S. Puijman near Wedde (the Netherlands). The studied feathers were

from specimens in the bird collection of the Groningen University (curator, S. Ackermann) and the Ecodrome museum (Zwolle, The Netherlands; curator, G. Beersma).

Scanning electron microscopy (SEM) on barb sections was performed with a Philips XL-30 ESEM. The images of the back and tail feather barbs, containing spongy structures, were Fourier transformed using Matlab or ImageJ.

Reflectance spectra of large feather areas were measured with an integrating sphere (AvaSphere-50-Refl; Avantes, Eerbeek, Netherlands). The light source was a halogen–deuterium lamp and the reflected light was collected by a photodiode array spectrometer (AvaSpec-2048-2; Avantes). A white diffusing reflectance standard (WS-2; Avantes) served as the reference.

Reflectance spectra of small barb areas (size, ~5–10 µm) were measured with a microspectrophotometer, i.e. a microscope (Olympus 20× objective, NA 0.46) with an adjustable measurement diaphragm, connected to the Avantes spectrometer.

Angle-dependent reflectance spectra were measured with a setup consisting of two fibres rotating independently from each other around the same axis in a plane containing the barb axis. One fibre, delivering light from a xenon lamp, illuminated an area with diameter ~4 mm; the other fibre captured the reflected light and delivered it to the spectrometer (see also Stavenga et al., 2011).

The feather barbs were further examined with an imaging scatterometer (Stavenga et al., 2009). The barbs were locally illuminated (spot size diameter, ~10 µm), and the light scattered into a 180 deg hemisphere was recorded.

### RESULTS

#### Feather colours

The common kingfisher, *A. atthis*, has an orange breast, a mostly cyan back (mantle) and a blue tail; the wings and head have a mix of blue and blue–green feather patches (Fig. 1A). The feathers strongly overlap (Fig. 1B), and all three main feather types (orange,

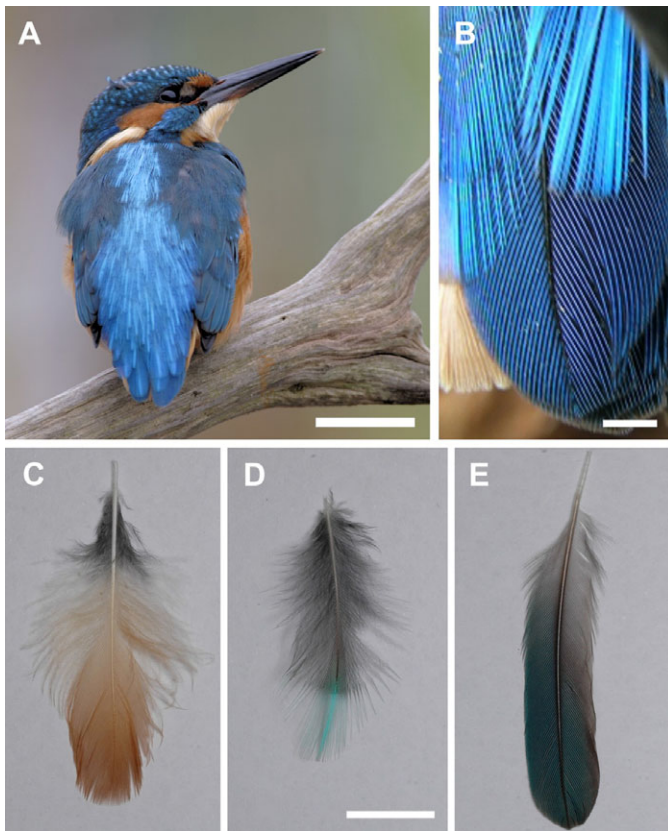


Fig. 1. The common kingfisher, *Alcedo atthis*, and its three main feather types. (A) The colourful bird with orange feathers at the breast, cyan feathers at the back and blue feathers at the tail. (B) Overlapping back and tail feathers. (C) A breast feather, which has mainly orange-coloured barbs, but also orange barbules. (D) A back feather, which has cyan-coloured barbs in the tip region of the feather. (E) A tail feather, which has blue-coloured barbs in a large part of the feather. All feather types have greyish barbs and barbules in the basal areas, near the quill. Scale bars: 5 cm (A), 0.2 cm (B) and 1 cm (C–E).

cyan and blue; Fig. 1C–E) are only coloured in fairly restricted tip areas, i.e. the areas that are exposed. The feather areas in the plumage that are covered by other feathers are greyish-black. Inspection with a light microscope revealed it is the feather barbs that are distinctly coloured, while the rachis and barbules are either whitish or grey, except for the tip area of the orange feathers, where the barbules are also coloured.

We measured the reflectance spectra of the tip areas of the three feather types with an integrating sphere (Fig. 2). The reflectance of the orange feathers is low in the short-wavelength range and high at long wavelengths, suggesting the presence of a pigment selectively absorbing in the shorter wavelength range, below 600 nm. The spectra of the cyan and blue feathers are quite different, with high reflectance below 500 nm and low reflectance above 600 nm. The cyan and blue spectra therefore probably have a structural basis. The spectral reflectance of the grey, non-coloured areas was in all three cases small, slightly increasing with wavelength, typical for melanin.

#### Feather barb structure

We applied SEM to reveal the structure of the feather barbs. The barbs appear to be compartmentalised into cells enveloped by a cortex (Fig. 3). The cellular compartments of the orange breast

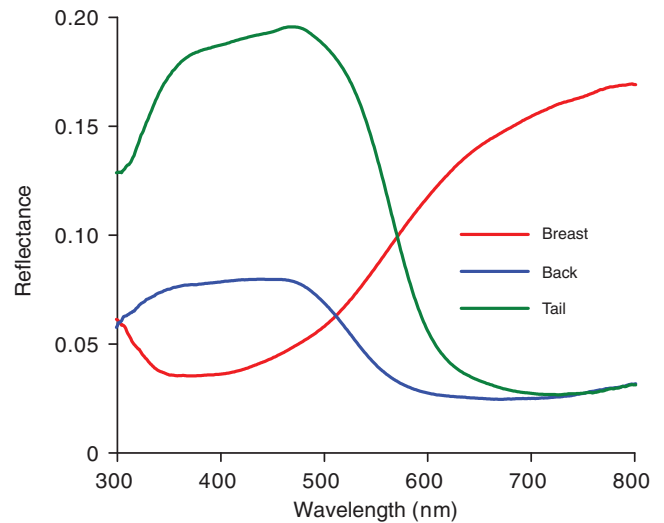


Fig. 2. Reflectance spectra of the coloured parts of the three feather types of Fig. 1, measured with an integrating sphere, using a white diffuser as reference.

feather barbs are hollow (Fig. 3A–C). Attached to the cell walls, small (<0.5 μm) granules are seen, which presumably contain the pigment responsible for the orange colouration. In contrast, the barbs of the other feather types contain spongy-structured cells with a central vacuole (Fig. 3D–F). The marked differences in anatomy suggest that the different barb structures underlie the different colour appearances of the feathers.

Structural colouration requires some order or periodicity of the light-reflecting and -scattering structures. We investigated whether the sponge cells in the barbs of both the cyan back feathers and blue tail feathers are ordered by applying a fast Fourier transform (FFT) to SEM images of planar sectioned spongy structures. The barbs of both feather types appeared to be amorphous with a short-range order (Fig. 4A,B), but the dimensions of the spongy structures differ slightly, as indicated by their Fourier power spectra (Fig. 4C,D). The ring diameters in the FFT patterns of the cyan back feather barb and the blue tail feather barb correspond to spatial distances of  $211 \pm 9$  nm and  $187 \pm 7$  nm, respectively. This conforms with the cut-off of the back feather's reflectance spectrum being at a longer wavelength compared with that of the tail feather (half-maximal values, ~570 and 550 nm, respectively).

To ascertain whether the sponge structures inside the barb cortex are the source of the colouration, we observed a back feather barb with an epi-illumination light microscope, using a linear polariser in the incident beam (Fig. 5). With a parallel analyser, the barb had a blue–green, spotty appearance, with a central, whitish line, presumably due to surface reflections. With a crossed analyser, the line vanished but the main barb colour simultaneously changed to dark blue (Fig. 5B). Apparently, the light reflected by the barb interior was partly depolarised, and predominantly so for the shorter wavelengths. That the coloured reflections originate from the sponge cells was demonstrated by cutting the barb and exposing the cut-end to xylene, a fluid with a refractive index close to that of the barb material. The xylene rapidly invaded the barb, presumably due to capillary forces. Within 1 min the coloured reflections separated into small patches. With a parallel polariser and analyser the colour of the reflected light was found to be blue–green (Fig. 5C), but with a crossed polariser and analyser the cells became bluish (Fig. 5D). After a few more minutes the

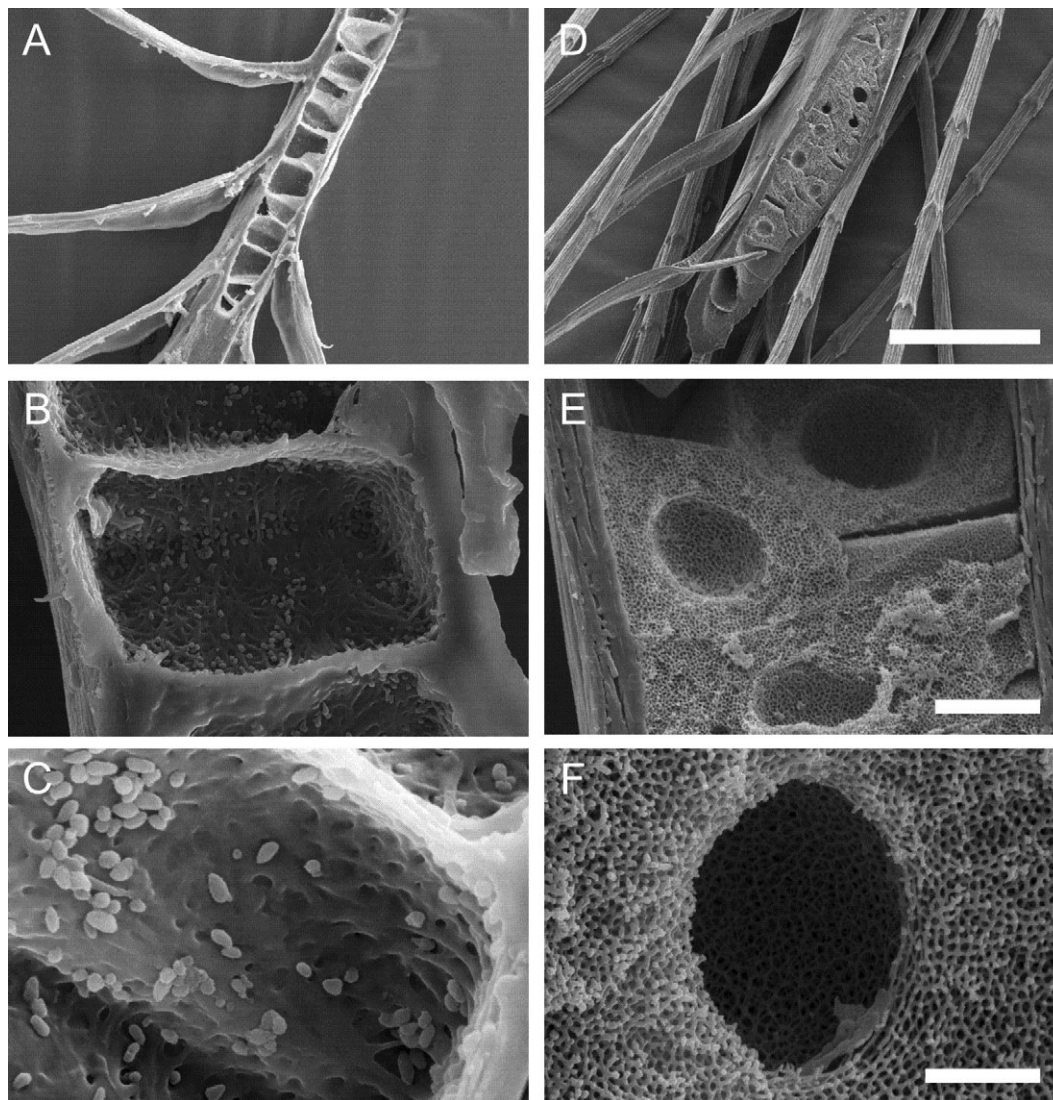


Fig. 3. Scanning electron micrographs (SEMs) of sectioned barbs of breast and tail feathers. (A) A sectioned barb of a breast feather with a few barbules. A thick cortex envelopes hollow cells. (B) Close up of a single cell. Small pigment granules are recognisable. (C) The pigment granules are attached to the cell walls. (D) A sectioned barb of a tail feather with several barbules. A number of sponge cells are surrounded by the barb cortex. (E) In the centre of the sponge cells there exists a large vacuole, a remnant of a nucleus, which in the cut cell is seen as a suppression. (F) Close up of a cut vacuole and the surrounding spongy structures. Scale bars: 50  $\mu\text{m}$  (A, D), 5  $\mu\text{m}$  (B, E), 2  $\mu\text{m}$  (C, F).

coloured reflections vanished. The xylene evidently reduced the refractive index contrast in the sponges and thus ultimately annihilated the reflections.

The different sponge cells in the same barb did not all have the same colour, and occasionally fully aberrant coloured cells were encountered (Fig. 6A). Also, the cells were not homogeneously coloured. With proper focusing of the microscope the vacuoles could be recognised as dark areas with a bright centre (Fig. 6A). Nevertheless, the reflectance spectra of the differently coloured cells, measured with a microspectrophotometer, had a similar shape and appeared to be simply shifted along the wavelength scale (Fig. 6B). In the back and tail feathers, the barb tips have approximately the same colour. The small, light coloured feathers of the kingfisher's head, however, have a central area where the barbs are bluish-green and towards the tips the barbs gradually become reddish (Fig. 6C). Indeed, reflectance spectra from barb areas in the central and tip region showed a distinct peak shift (Fig. 6D), indicating that the head feather barb tips also contain spongy structures.

#### Feather iridescence

Generally, pigment-coloured substances scatter light diffusely and structurally coloured materials exhibit directional reflections. We

investigated the spatial aspects of the light reflected by the feather barbs with an imaging scatterometer, which provides images of the light scattered (or reflected) in the hemisphere above the illuminated object. A small area (diameter,  $\sim 5 \mu\text{m}$ ) was illuminated by a white light beam with a narrow aperture of  $\sim 5$  deg. The longitudinal axis of the barbs was oriented horizontally. In the case of an orange breast feather barb (Fig. 7A), orange light was scattered into virtually the full hemisphere, showing that the barb approximated a diffuser. However, superimposed on the wide-angle scattering a vertical whitish line emerged, due to reflections from the barb cortex. The vertical line featured interference patterns, indicating that the cortex acts as a thin film (see below). Fig. 7B–D show scatterograms of a blue tail feather barb, a cyan back feather barb and the red tip of a head feather barb. The spatial scattering, although spotty, was also wide angled, but the angular profile was wavelength dependent, with a larger angular spread occurring for the shorter wavelengths. In these cases too, a whitish, vertical line, due to cortex reflections, was superimposed on the coloured scattering. The cortex reflection lines did not always cover the full hemisphere (Fig. 7B–D), indicating that the barbs were not smooth circular cylinders.

The spongy barbs were clearly iridescent. We measured the angular dependence of the reflectance spectra of the tip area of a

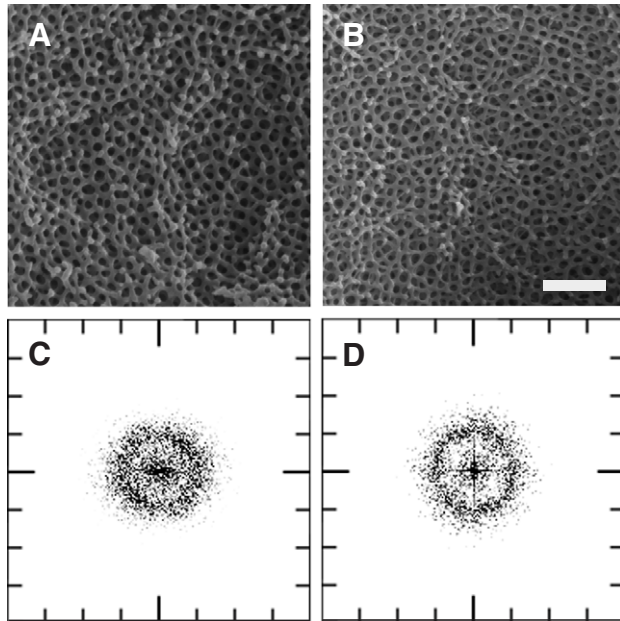


Fig. 4. Scanning electron microscopy and Fourier transforms of the planar sectioned spongy structures of the cyan back and blue tail feathers. (A) SEM of the spongy structure of the back feather. (B) SEM of the spongy structure of the tail feather. (C) Power spectrum of the back feather sponge of A calculated with a fast Fourier transform (FFT). (D) FFT of the tail feather sponge. Scale bar:  $1\ \mu\text{m}$  (A,B). In C and D, the unit distance represents a spatial frequency of  $0.005\ \text{nm}^{-1} = 5\ \mu\text{m}^{-1}$ .

back feather with a setup that consists of two coaxially rotating optical fibres (Fig. 8A). The feather was positioned so that the rotation axis was in the feather plane, perpendicular to the barbs. The spectra were measured while always applying the same, normal illumination; that is, the angle of light incidence was  $\theta=0^\circ$  (Fig. 8A, inset). The angle,  $\phi$ , of the detection fibre, rotating in a plane parallel to the longitudinal axes of the barbs, was varied. The

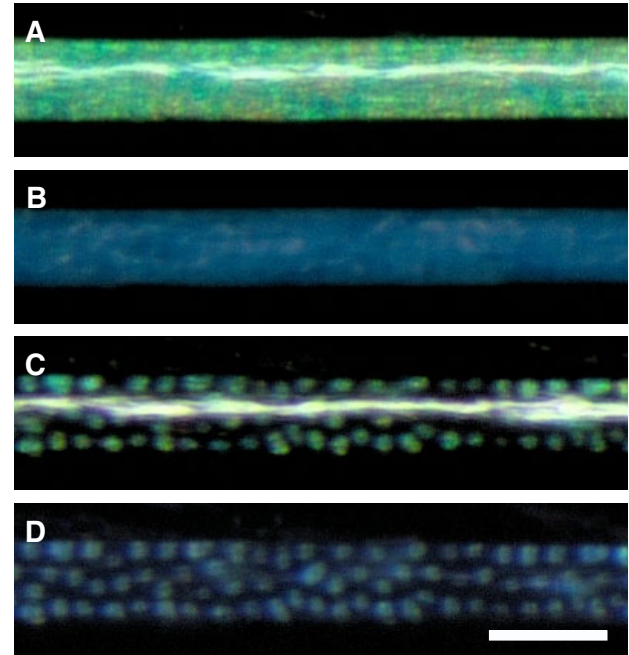


Fig. 5. Dry and wetted back feather barb observed with polarised light. (A) A dry barb illuminated with linear polarised light with a parallel analyser, showing the non-homogeneous colouration of the barb interior together with the whitish surface reflection. (B) The dry barb observed with a crossed polariser and analyser, showing a much bluer colour of the interior and extinction of the surface reflection. (C) After immersion with xylene for several minutes, observed with the parallel polariser and analyser, the surface reflection is unchanged, but the reflection from the interior is resolved into isolated patches representing single cells. (D) As in C but with the crossed polariser and analyser, showing a much bluer reflection, as in B. Scale bar for A–D:  $50\ \mu\text{m}$ .

shape of the reflectance spectrum gradually changed with an increase of the scattering angle, with the peak shifting to shorter wavelengths (Fig. 8A; compare also Fig. 7B–D).

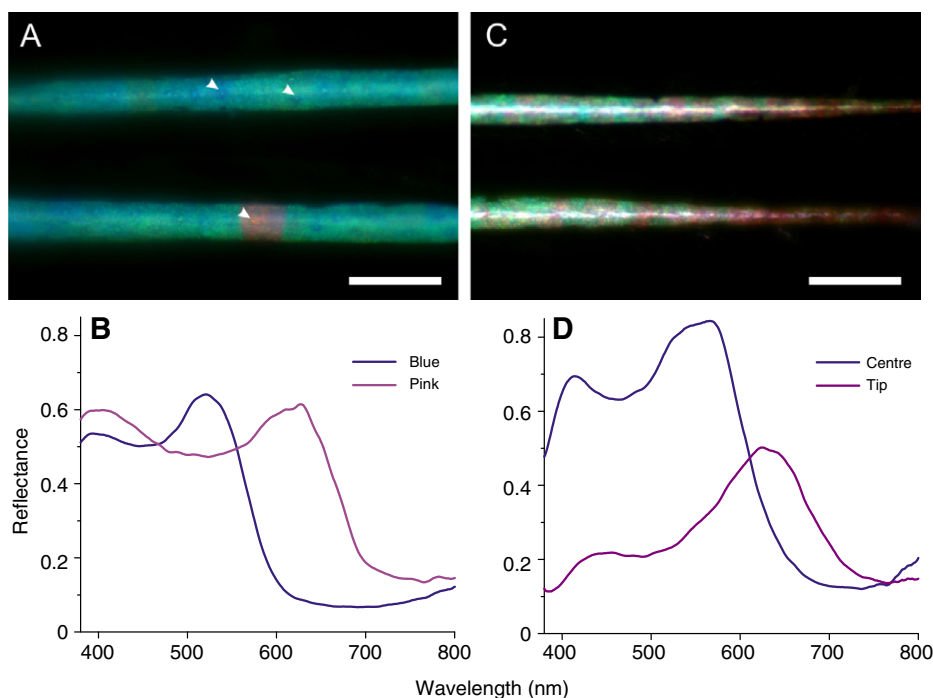


Fig. 6. Variations in the structural colouration of the barbs. (A) Back feather barbs with mainly similar bluish coloured cells. Occasionally an aberrant cell with a different colour (here pinkish) occurs. The vacuoles are distinguishable as dark areas with a central bright spot (arrowheads). Bar:  $50\ \mu\text{m}$ . (B) Reflectance spectra measured from small areas ( $\sim 5 \times 5\ \mu\text{m}^2$ ) of the blue and pink areas of the barbs in A. (C) Barbs of a head feather area (left), but towards the tip the colour becomes reddish. Bar:  $100\ \mu\text{m}$ . (D) Reflectance spectra from the central (C, left) and tip (C, right) area of the head feather barbs.

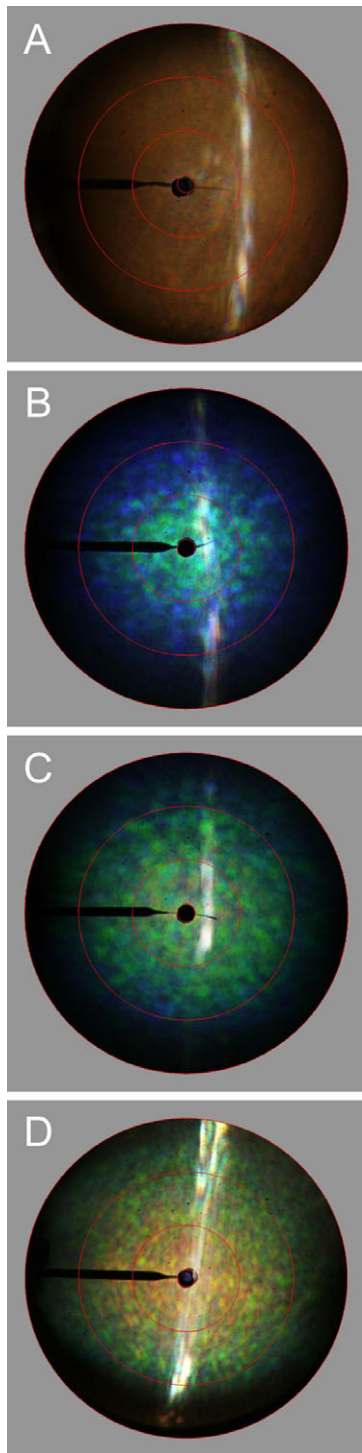


Fig. 7. Scatterograms of the coloured feather barbs. The barbs were oriented horizontally. (A) Diffuse orange scatter pattern of a breast feather barb, together with a locally coloured vertical line created by cortex reflections. (B) Spotty scatter pattern of a tail feather barb, scattering greenish light into near-normal directions and scattering bluish light at larger angles, together with the cortex reflection line. (C) A similar spotty scatter pattern of a back feather barb with green scattered light extending over a smaller spatial angle than blue scattered light. (D) Scatter pattern from the reddish tip of a head feather barb, with red–orange scattering in a restricted spatial angle and green scattering in a larger spatial angle. The shadow of the glass pipette holding the barb is seen at 9 o'clock. The red circles indicate angles of 5, 30, 60 and 90 deg. The black centre is due to the central hole in the ellipsoid mirror of the scatterometer.

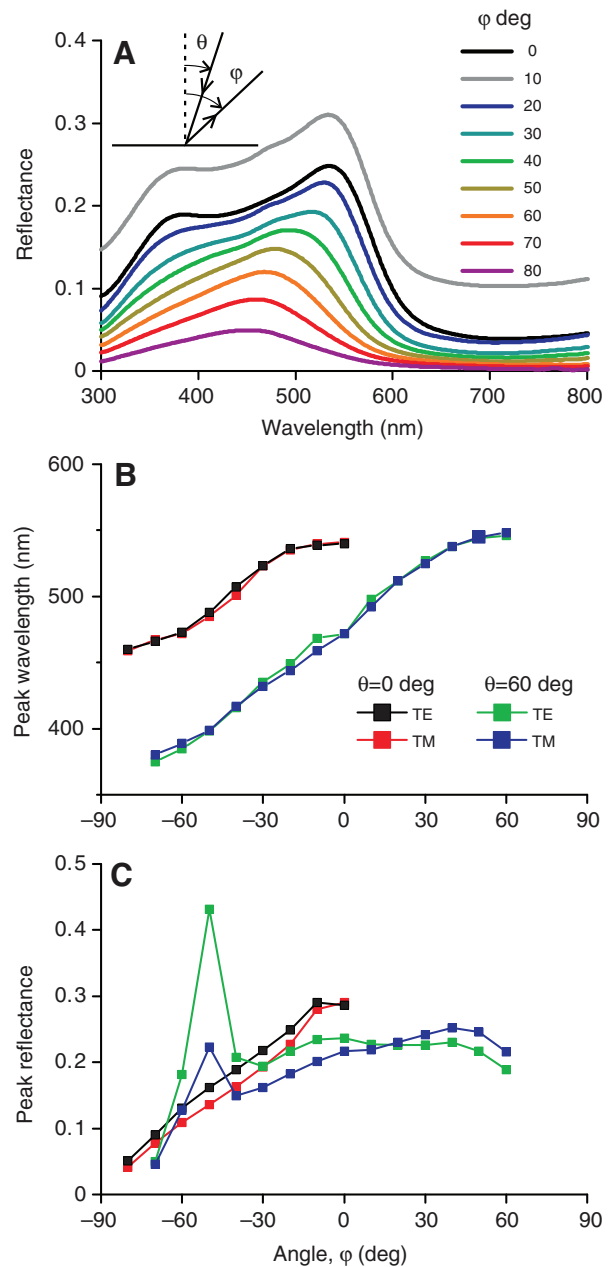


Fig. 8. Angle dependence of the reflectance of the tip area of a back feather, measured with a setup consisting of two rotatable optical fibres. (A) The angle of the illumination fibre was stable, with direction about normal to the feather surface ( $\theta=0$  deg); the angle of the detector fibre,  $\varphi$ , was varied (inset). The incident light was unpolarised. The reflectance spectrum shifted increasingly towards shorter wavelengths with an increase of the detection angle. (B) Dependence of the reflectance peak wavelength for s- (or TE-) and p- (or TM-) polarised light with normal ( $\theta=0$  deg) and oblique illumination ( $\theta=60$  deg). (C) Dependence of the peak reflectance for s- (or TE-) and p- (or TM-) polarised light with normal ( $\theta=0$  deg) and oblique illumination ( $\theta=60$  deg).

Repeating the same measurement with a polarisation filter in front of the detection fibre yielded very similar reflectance spectra for s- (or TE-) and p- (or TM-) polarised light at all detection angles; the peak wavelength (Fig. 8B) and the amplitude (Fig. 8C) had approximately the same angle dependence. Also, when the angle of light incidence was changed to  $\theta=60$  deg, the reflectance spectra

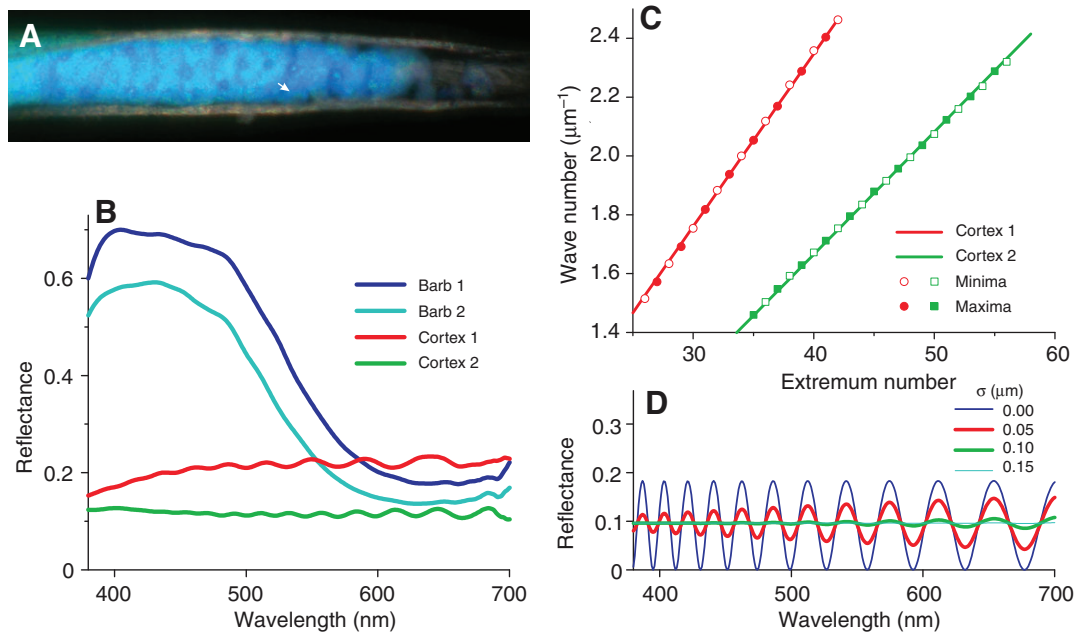


Fig. 9. Reflectance properties of a tail feather barb. (A) A very obliquely sectioned barb, showing loosened cells enveloped by the barb cortex. Bar: 50  $\mu\text{m}$ . (B) Reflectance spectra measured with a microspectrophotometer from a small area ( $\sim 5 \times 5 \mu\text{m}^2$ ) of undamaged barbs (barb 1 and barb 2) and of the cortex, i.e. where the sponge cells were absent (cortex 1 and cortex 2). (C) The wave number (that is, the inverse wavelength) of the extrema of the cortex reflectance spectra of B plotted as a function of the extremum number, which was deduced from a linear fit. (D) Reflectance spectra calculated for a thin layer (in air), having a refractive index of 1.58 and a Gaussian distributed thickness, with mean  $d=3 \mu\text{m}$  and standard deviation  $\sigma=0, 0.05, 0.10$  and  $0.15 \mu\text{m}$ . The amplitude of the oscillating reflectance decreases with increasing  $\sigma$  and increases with increasing wavelength (when  $\sigma>0$ ).

obtained for TE- and TM-polarised light hardly differed at all detection angles (Fig. 8B,C). Interestingly, the reflectance showed a sudden high maximal value for a detection angle value  $\varphi \approx -50$  deg; that is, when  $\varphi = -\theta + \gamma$ , where  $\gamma \approx 10$  deg is the local tilt angle of the feather barbs. The peak resulted from the specularity of the cortex (visible as the white line in Fig. 7B–D).

#### Barb cortex acting as a thin film

To further investigate the separate contributions of the sponge cells and the enveloping cortex to the reflectance measurements, we obliquely sectioned a tail feather barb. This showed the sponge cells as irregularly shaped, coloured blocks within the cortex (Fig. 9A; see also Fig. 3E). The reflectance spectra measured with a microspectrophotometer from the exposed sponge cells slightly varied in amplitude and spectral location (Fig. 9B; see also Fig. 6). In the sectioned barbs not only coloured sponge cells became exposed but also cells with grey–black melanin pigments, positioned below the sponge cells. The latter clearly serve as an absorbing layer below the sponge cells, so as to enhance colour contrast.

The spectra measured from larger areas of isolated cortex, of  $>10 \mu\text{m}$  in size, were more or less flat, but small areas featured periodic oscillations, which increased in amplitude with increasing wavelength (Fig. 9B). The oscillations were sometimes also easily recognisable in the spectra of intact barbs and thus demonstrate that the cortex acts locally as a thin film.

It is well known that the reflectance spectrum of a thin film with thickness  $d$  and refractive index  $n$  has extrema (minima and maxima) for wavelengths  $\lambda_{u_i} = c/u_i$ , where  $c$  is a constant and  $u_i > 0$  and an integer (minima for even values of  $u$  and maxima for odd values of  $u$ ). The constant  $c = 4nd \cos \theta$ , where  $\theta$  is the angle of light incidence, reduces to  $c = 4nd$ , because in the reflectance

measurements of Fig. 9B,  $\theta \approx 0$  deg. We evaluated the wavelengths of the extrema in the cortex spectra of Fig. 9B and plotted their inverse values in Fig. 9C as a function of their extremum number  $u_i$ ; the value of the extremum numbers was deduced with the assumption that the inverse wavelengths have to fit a linear function:  $1/\lambda_{u_i} = u_i/c$ . The slope of the linear function,  $1/c = 1/(4nd)$ , yielded the thickness,  $d$ , of the cortex by using the refractive index value  $n = 1.58$  (Brink and van der Berg, 2004). We thus derived that the thicknesses of cortex 1 and 2 (Fig. 9B,C) were  $2.7 \pm 0.1 \mu\text{m}$  and  $3.8 \pm 0.1 \mu\text{m}$ , respectively, in fair agreement with the SEM images (Fig. 3).

For an ideal thin film, the amplitude of the oscillations is constant, but the amplitude of the cortex spectra increased with increasing wavelength (Fig. 9B). This indicates that the cortex thickness in the measurement areas was not constant. We investigated the effect of a non-constant thin film thickness in Fig. 9D by assuming a Gaussian-distributed thickness with mean  $3.0 \mu\text{m}$  and standard deviation  $\sigma = 0.0, 0.05, 0.10$  and  $0.15 \mu\text{m}$ . In the first case, representing an ideal thin film, the amplitude of the oscillating reflectance spectrum is constant. With increasing  $\sigma$  the amplitude decreases and becomes wavelength dependent, increasing with increasing wavelength. The amplitude of the extrema becomes negligible when  $\sigma > 0.15 \mu\text{m}$  (Fig. 9D). The calculations show that a variation of the thickness of only a few percent is sufficient to create the wavelength-dependent amplitude and at the same time severely reduce the amplitude of the oscillating reflectance spectrum. The two different cortex spectra of Fig. 9B as well as the anatomical data indicate that the cortex thickness varies considerably, and therefore the thin-film characteristics will only be recognised in microspectrophotometrical measurements from (very) small areas.

## DISCUSSION

The chemical and physical colouration mechanisms of birds are in principle the same as those applied by other living systems. Pigments, used for chemical colouration, are often deposited in granules, and therefore the granules attached to the walls of the hollow cells of the orange breast feather barbs most probably contain a short-wavelength-absorbing pigment (Fig. 3B,C). The very irregular spatial organisation of the barb cells causes randomisation of the direction of incident light, resulting in diffuse scattering of the little-absorbed long-wavelength light (Fig. 7A).

Although the spatial organisation of the sponge cells inside the kingfisher's back and tail feather barbs is irregular (Fig. 4A,B), there still exists sufficient quasi-order (Fig. 4C,D) to create structural colouration, which changes in hue when observed from different directions (Fig. 7). The spectral peak depends on the dimensions of the sponge structures (Dyck, 1971; Finger, 1995; Shawkey et al., 2009). Spongy barbs are widespread among birds (Prum et al., 1999; Shawkey et al., 2003; Prum, 2006; Shawkey et al., 2006), but so far the optics of the sponge structures have evaded ready analysis because of the complexity of the structures and the deviations from regularity (Prum, 2006). Important progress has recently been made, however (Noh et al., 2010a; Noh et al., 2010b).

Many birds have iridescent feathers due to regularly structured barbules (Durrer, 1977; Kinoshita and Yoshioka, 2005; Prum, 2006; Yoshioka et al., 2007; Kinoshita, 2008; Stavenga et al., 2010). An extensively investigated case is that of the neck feathers of pigeons, which were demonstrated to be coloured as a result of light interference in the barbule cortex, which envelopes heavily melanin-pigmented cells (Yoshioka et al., 2007; Nakamura et al., 2008). Interestingly, the reflectance spectra measured from the pigeon feather barbules showed oscillations, which increased in amplitude with increasing wavelength (Osorio and Ham, 2002; Nakamura et al., 2008). This phenomenon was explained by assuming that in the sampled area the cortex acted as a thin film with a non-constant thickness (Nakamura et al., 2008). The oscillations in the pigeon spectra are very similar to those of the cortices of the common kingfisher's barbs (Fig. 9B). We also have concluded that a non-constant cortex thickness is the most likely explanation for the increasing amplitude of the oscillations with increasing wavelength (Fig. 9D).

In the modelling of Fig. 9D, we assumed normal illumination, but the aperture of the microspectrophotometer objective used for measuring the reflectance spectra was not negligible, so the assumption of normal light incidence,  $\theta=0$  deg, might not be fully justified. Further modelling showed that the objective aperture only very slightly affected the modulations of the reflectance spectra. Also, the reflected light captured by the objective depends on the shape of the reflecting object. For instance, the local curvature of the cortex will determine how much light is captured by the objective aperture. Small irregularities in the cortex will therefore cause spatial reflection profiles that affect the reflectance spectrum (Fig. 9B). We note that the reflectance spectra are measured relative to a white diffuser, which tends to overestimate the reflectance of a mirror-like object.

Generally, the cortex will contribute noticeably to the total barb reflectance, especially with oblique illumination (Fig. 8C). The cortex contribution will be more or less wavelength independent in measurements from areas with diameter  $>10\mu\text{m}$ . The cortex reflectance then forms an approximately constant background in the reflectance spectra from intact barbs (Fig. 2, Fig. 9B). Possibly the distinct reflectance at wavelengths  $>600\text{nm}$  in the experimentally measured spectrum of bluebird feathers (Shawkey et al., 2009) is mainly due to the background reflectance contributed by the barb cortices.

The dependence of feather colours on illumination and viewing angles has been explored in several bird species (Osorio and Ham, 2002). Structural coloured feathers commonly exhibit iridescence because of the interference of light in the periodic structures. Iridescence occurs when applying illumination with a narrow-aperture light source (Fig. 7, Fig. 9B,C), but the feathers appear non-iridescent under omni-directional illumination, because of the isotropic nature of the sponges (e.g. Noh et al., 2010a). In the case of the plumage of intact birds, the reflectance spectra will be similar to those of the measured barbs because only the tip areas of the feathers are exposed. The feather iridescence of birds in the natural habitat, with wide-field illumination, will no longer be prominently visible (Osorio and Ham, 2002).

## CONCLUSIONS

The bright colours of the common kingfisher *A. atthis* are created by two types of feather barb: one filled with pigment granules and the other with quasi-ordered channel-type keratinous sponges. A broad-band background reflection is added by the cortex of the shiny feathers, especially when the feathers are illuminated from oblique directions.

## ACKNOWLEDGEMENTS

Drs M. D. Shawkey and H. Ghiradella read a preliminary version of the manuscript.

## FUNDING

This study was supported by the Air Force Office of Scientific Research/European Office of Aerospace Research and Development (AFOSR/EOARD) [grant FA8655-08-1-3012].

## REFERENCES

- Brink, D. J. and van der Berg, N. G. (2004). Structural colours from the feathers of the bird *Bostrychia hagedash*. *J. Phys. D Appl. Phys.* **37**, 813-818.
- D'Alba, L., Saranathan, V., Clarke, J. A., Vinther, J. A., Prum, R. O. and Shawkey, M. D. (2011). Colour-producing  $\beta$ -keratin nanofibres in blue penguin (*Eudyptula minor*) feathers. *Biol. Lett.* **7**, 543-546.
- Doucet, S. M. and Meadows, M. G. (2009). Iridescence: a functional perspective. *J. R. Soc. Interface* **6**, S115-S132.
- Durrer, H. (1977). Schillerfarben der Vogelfeder als Evolutionsproblem. *Denkschr. Schweiz. Naturforsch. Ges.* **91**, 1-126.
- Dyck, J. (1971). Structure and colour-production of the blue barbs of *Agapornis roseicollis* and *Cotinga maynana*. *Z. Zellforsch.* **115**, 17-29.
- Finger, E. (1995). Visible and UV coloration in birds: Mie scattering as the basis of color in many bird feathers. *Naturwissenschaften* **82**, 570-573.
- Hill, G. E. and McGraw, K. J. (2006). *Bird Coloration*, Vol. 1, *Mechanisms and Measurements*. Cambridge: Harvard University Press.
- Kinoshita, S. (2008). *Structural Colors In The Realm Of Nature*. Singapore: World Scientific.
- Kinoshita, S. and Yoshioka, S. (2005). Structural colors in nature: the role of regularity and irregularity in the structure. *Chemphyschem.* **6**, 1-19.
- McGraw, K. J. (2006). The mechanics of uncommon colors in birds: pterins, porphyrins, and psittacofulvins. In *Bird Coloration*, Vol. 1, *Mechanisms and Measurements* (ed. G. E. Hill and K. J. McGraw), pp. 354-398. Cambridge: Harvard University Press.
- Nakamura, E., Yoshioka, S. and Kinoshita, S. (2008). Structural color of rock dove's neck feather. *J. Phys. Soc. Jpn.* **77**, p. 124801.
- Noh, H., Liew, S. F., Saranathan, V., Mochrie, S. G. J., Prum, R. O., Dufresne, E. R. and Cao, H. (2010a). How noniridescent colors are generated by quasi-ordered structures of bird feathers. *Adv. Mater.* **22**, 2871-2880.
- Noh, H., Liew, S. F., Saranathan, V., Prum, R. O., Mochrie, S. G. J., Dufresne, E. R. and Cao, H. (2010b). Double scattering of light from biophotonic nanostructures with short-range order. *Opt. Express* **18**, 11942-11948.
- Osorio, D. and Ham, A. D. (2002). Spectral reflectance and directional properties of structural coloration in bird plumage. *J. Exp. Biol.* **205**, 2017-2027.
- Prum, R. O. (2006). Anatomy, physics, and evolution of avian structural colors. In *Bird Coloration*, Vol. 1, *Mechanisms And Measurements* (ed. G. E. Hill and K. J. McGraw), pp. 295-353. Cambridge: Harvard University Press.
- Prum, R. O., Torres, R., Williamson, S. and Dyck, J. (1999). Two-dimensional Fourier analysis of the spongy medullary keratin of structurally coloured feather barbs. *Proc. R. Soc. Lond. B* **266**, 13-22.
- Prum, R. O., Dufresne, E. R., Quinn, T. and Waters, K. (2009). Development of colour-producing beta-keratin nanostructures in avian feather barbs. *J. R. Soc. Interface* **6**, S253-S265.
- Shawkey, M. D., Estes, A. M., Siefferman, L. M. and Hill, G. E. (2003). Nanostructure predicts intraspecific variation in ultraviolet-blue plumage colour. *Proc. R. Soc. B* **270**, 1455-1460.

- Shawkey, M. D., Balenger, S. L., Hill, G. E., Johnsen, L. S., Keyser, A. J. and Siefferman, L.** (2006). Mechanisms of evolutionary change in structural plumage coloration among bluebirds (*Sialia spp.*). *J. R. Soc. Interface* **3**, 527-532.
- Shawkey, M. D., Saranathan, V., Pálsdóttir, H., Crum, J. C., Auer, M. L. and Prum, R. O.** (2009). Electron tomography, 3D Fourier analysis and color prediction of a 3D bio-photonic nanostructure. *J. R. Soc. Interface* **6**, S213-S220.
- Srinivasarao, M.** (1999). Nano-optics in the biological world: beetles, butterflies, birds and moths. *Chem. Rev.* **99**, 1935-1961.
- Stavenga, D. G., Leertouwer, H. L., Pihl, P. and Wehling, M. F.** (2009). Imaging scatterometry of butterfly wing scales. *Opt. Express* **17**, 193-202.
- Stavenga, D. G., Leertouwer, H. L., Marshall, N. J. and Osorio, D.** (2010). Dramatic colour changes in a bird of paradise caused by uniquely structured breast feather barbules. *Proc. R. Soc. B* **278**, 2098-2104.
- Stavenga, D. G., Wilts, B. D., Leertouwer, H. L. and Hariyama, T.** (2011). Polarized iridescence of the multilayered elytra of the Japanese Jewel Beetle, *Chrysochroa fulgidissima*. *Phil. Trans. R. Soc. B* **366**, 709-723.
- Vukusic, P. and Sambles, J. R.** (2003). Photonic structures in biology. *Nature* **424**, 852-855.
- Yoshioka, S., Nakamura, E. and Kinoshita, S.** (2007). Origin of two-color iridescence in rock dove's feather. *J. Phys. Soc. Jpn.* **76**, p. 013801.